



In Silico Docking Analysis of Phytochemicals from Chili (*Capsicum Frutescens*) Leaves Against Breast Cancer Targets

Nyque L. Chu¹, Flexzie Coleen B. Cosmo², Jerome Satriani S. Orosio³

^{1,2,3} UG Student, Davao City National High School, F. Torres St., Davao City

DOI : <https://doi.org/10.55248/gengpi.6.0425.1316>

ABSTRACT

Breast cancer poses a significant global public health threat due to its high incidence, mortality rates, and the growing resistance to conventional treatments, necessitating the development of more effective therapies. This study focuses on the molecular docking analysis of 30 phytochemicals from chili leaves (*Capsicum frutescens*) against Estrogen Receptor Alpha (PDB: 3ERT) and Estrogen Receptor Beta (PDB: 5TOA) using Autodock Vina. The results revealed that Apigenin is the most promising ligand for ER α , exhibiting the strongest binding affinity (-8.0 kcal/mol), while Cyanidin showed a strong binding affinity of -8.4 kcal/mol for ER β . All analyzed phytochemicals interacted with crucial binding residues on 3ERT and 5TOA, demonstrating potential as inhibitors of both targets. These findings highlight the potential of chili leaf phytochemicals as inhibitors of breast cancer proteins, providing valuable insights into drug development. Further research and experimental validation are needed to develop natural compound-based therapies against breast cancer, underscoring the significance of molecular docking in identifying potential candidates for drug discovery.

KEYWORDS: *Breast cancer, Molecular Docking, Estrogen Receptor Alpha, Estrogen Receptor Beta, Capsicum frutescens, 3ERT, 5TOA*

Introduction

Breast cancer is a condition where abnormal breast cells multiply uncontrollably, forming tumors. If untreated, these tumors can spread to other parts of the body and become life-threatening (World Health Organization: WHO, 2024a). Breast cancer is one of the most prevalent cancers among women and individuals assigned female at birth (AFAB). It occurs when cancer cells in the breast multiply and form tumors. Around 80% of breast cancer cases are invasive, meaning the tumor can spread from the breast to other parts of the body. While breast cancer mainly affects women aged 50 and older, it can also occur in younger women and AFAB individuals. Additionally, men and those assigned male at birth (AMAB) can develop breast cancer as well (Breast Cancer, 2024)

According to Menon et al. (2024), breast cancer is the most frequently diagnosed cancer in women, making up over 1 in 10 new cancer cases each year. Globally, it is the second leading cause of cancer-related deaths among women. In 2022, 2.3 million women worldwide were diagnosed with breast cancer, leading to 670,000 deaths. Breast cancer can occur in women of any age after puberty, with the likelihood increasing as they age. Global data highlights significant disparities in breast cancer impact based on a country's level of development. In countries with a very high Human Development Index (HDI), 1 in 12 women is diagnosed with breast cancer in their lifetime, and 1 in 71 women die from it. Conversely, in countries with a low HDI, although only 1 in 27 women is diagnosed with breast cancer, 1 in 48 women die from it (World Health Organization: WHO, 2024b). According to the WHO, the Philippines had 33,079 new cases of breast cancer in 2022, one of the highest rates in Asia. Data from the Philippine Cancer Society and the Department of Health's Rizal Cancer Registry in 2009 reported 1,615 breast cancer patients and observed an increase in cases from 1980 to 2002.

The exact cause of most breast cancers is unknown, but researchers have identified factors that can increase risk, such as hormones, lifestyle choices, and environmental influences. The development of breast cancer is thought to involve a complex interaction between genetics and the environment. Breast cancer begins when changes in the DNA of breast cells disrupt normal growth and death patterns. Healthy cells grow and divide at a controlled rate and die at a set time.

In cancer cells, DNA changes cause uncontrolled growth and prevent normal cell death, leading to an excess of cells. These cancer cells can form a tumor, which may invade and damage nearby healthy tissue. Over time, cancer cells can spread to other parts of the body, a process known as metastatic cancer. Breast cancer often starts in the cells lining the milk ducts (invasive ductal carcinoma) or in the milk-producing lobules (invasive lobular carcinoma). It can also start in other breast cells, but this is less common. (Breast Cancer - Symptoms and Causes - Mayo Clinic, 2024). According to Website (2024), symptoms of breast cancer in women can include a lump or swelling in the breast, chest, or armpit, as well as changes in the skin of the breast, such as dimpling or redness. There may be a noticeable change in the size or shape of

one or both breasts. Nipple discharge that is not related to pregnancy or breastfeeding, particularly if it contains blood, can also be a sign. Changes in the nipple, such as it turning inward or developing a rash, might occur. Persistent pain in the breast or armpit is another potential symptom, although occasional breast pain is usually not linked to breast cancer.

Chili leaves also known as *Capsicum Frutescens* L. are a hidden culinary gem often overshadowed by their more famous relatives, chili peppers and cilantro. Despite being frequently overlooked, these versatile leaves add a unique flavor and texture to dishes, making them a valuable ingredient in various cuisines from Asia to Mexico. Originating from the same plant as chili peppers, chili leaves are dark green, elongated, and have pointed tips, similar in appearance to oversized bay leaves. The leaves can grow up to 12 cm long and 7.5 cm. They feature a slightly rough top surface, a smooth underside, and visible veins. When crushed or torn, they release a fragrant aroma reminiscent of fresh peppers, enhancing dishes with their distinctive flavor. Part of the *Capsicum* family, chili leaves are harvested while young, tender, and bright green. They offer a slightly bitter taste with varying hints of heat, depending on the quantity used. The leaves are notable for their high essential oil content, including capsaicin, which not only contributes to their flavor but also has anti-inflammatory properties when consumed in moderation (Kristine 2023a).

Despite advances in breast cancer treatment, such as surgery, chemotherapy, and radiation, these therapies often come with severe side effects and challenges related to drug resistance. Therefore, the search for new and effective treatment options continues. One promising area of research focuses on natural products, such as *Capsicum frutescens* L. (chili) leaves, which have been traditionally overlooked compared to their fruit counterparts. Chili leaves offer numerous health benefits that are still being discovered. Known scientifically as *Capsicum frutescens*, these leaves are a valuable source of various vitamins and can help prevent several illnesses. They are low in fat and calories, and can lower levels of bad cholesterol in the body. Chili leaves support metabolism by burning excess fat and converting it into energy. They are rich in nutrients and vitamins, including vitamins A and C, and contain high levels of antioxidants that protect against damage to nerves, cells, and blood vessels. (Homeshop.ph - your online grocery partner, n.d.).

Chili leaves not only enhance the flavor of various dishes but also offer a range of health benefits due to their rich nutrient content. They are packed with Vitamin C, which strengthens the immune system and reduces inflammation, and also contain Vitamins A and K, promoting healthy vision and bone strength. Additionally, research indicates that chili leaves have antibacterial properties that help combat harmful bacteria in the body. They are also a rich source of antioxidants, such as beta-carotene, which protect the body from damage (Kristine 2023b). Additionally, cayenne pepper (*Capsicum frutescens* L.) is a popular type of chili widely grown in Indonesia due to its health benefits and relatively high market value. The leaves of cayenne pepper have the potential to produce bioactive compounds, containing flavonoids, tannins, steroids/triterpenoids, alkaloids, and saponins. (Sabilu & Jafriati, 2023). Moreover, according to Batiha et al. (2020), the leaves of chili plants contain alkaloids, tannins, and flavonoids, while the roots are composed of steroids, alkaloids, coumarins, glycosides, and triterpenoids. In addition, *Capsicum annum* L. is abundant in antioxidants, alkaloids, flavonoids, polyphenols, carotenoids, as well as vitamins C and E. Capsaicin, the primary compound in cayenne pepper, is known for its pain-relieving and desensitizing effects, making it helpful in managing chronic pain linked to conditions such as rheumatoid arthritis, post-herpetic neuralgia, diabetic neuropathy, and other pain disorders. Additionally, it exhibits anti-inflammatory, bactericidal, antifungal, and anti-diabetic properties. (*Capsicum Frutescens* (Sili) – Herbanext Laboratories, Inc., n.d.)

The use of in-silico methods in drug development is expanding. Computational techniques simulate various aspects of drug discovery and development, such as virtual ligand screening, target and lead identification, and compound library creation. These techniques include databases, pharmacophores, homology models, quantitative structure-activity relationships, machine learning, data mining, network analysis tools, and computer-based data analysis.

Moreover, in-silico studies play a critical role in drug discovery by offering powerful tools for predicting the therapeutic potential of new drugs, reducing the time and resources required for development, and enhancing the overall likelihood of finding effective treatments (Roney & Aluwi, 2024).

In breast cancer treatment, the incorporation of molecular docking has emerged as a critical component in the drug discovery process. This computational method allows to systematically investigate the interactions between potential therapeutic compounds and specific target proteins associated with breast cancer. Molecular docking is a computational method used to predict the binding affinity between ligands and receptor proteins. While it shows promise in nutraceutical research, it has become a powerful tool in drug development. Nutraceuticals are bioactive compounds found in food that can be utilized for disease management. Identifying their molecular targets can aid in developing new therapies tailored to specific diseases. (Agu et al., 2023). Moreover, understanding binding affinity is crucial for grasping the intermolecular interactions that drive biological processes, structural biology, and the relationship between structure and function. It is also an essential aspect of drug discovery, as measuring binding affinity aids in designing drugs that selectively and specifically bind to their targets. (Malvern Panalytical, n.d.). Additionally, according to Asiamah et al. (2023) natural products have been traditionally used to treat various diseases, especially in developing countries. The recognition of compounds derived from natural sources as lead compounds for conventional drug development is well-established. In developing nations, drug discovery efforts involving natural products typically focus on using crude extracts in in-vitro and/or in-vivo assays, with fewer efforts directed toward isolating active compounds for structural studies. When pure secondary metabolites are isolated and their structures characterized, these studies often have limited bioactivity evaluations. In conventional drug discovery, molecular docking is a valuable tool for predicting how small molecules interact with drug targets, helping to guide synthesis decisions. Medicinal chemists use molecular docking to predict and synthesize compounds with potential pharmacological

activity, thereby saving time and reducing costs. Efforts are being made to integrate molecular docking techniques into natural product-based drug discovery.

The significance of this research lies in its potential to uncover new, plant-based breast cancer treatments that could be more effective and less harmful. It bridges traditional medicine with modern scientific evidence, offering valuable insights for oncology, natural medicine, and pharmacology researchers, as well as educators and students exploring the medicinal properties of plants.

This research investigates the inhibitory potential of selected phytochemicals derived from chili leaves (*Capsicum frutescens*) on Estrogen Receptor Alpha and Estrogen Receptor Beta, proteins associated with breast cancer, utilizing molecular docking analysis. The specific objectives of this study are as follows:

- I. Identify all of the phytochemicals present in *Capsicum frutescens* and evaluate the drug-likeness by employing pkCSM-pharmacokinetics and SwissADME to comply with the Lipinski Rule of Five.
- II. To evaluate and comprehend the binding interactions between the selected phytochemicals and the breast cancer's estrogen receptors alpha and beta using molecular docking simulations.
- III. To thoroughly examine the interactions displayed by the selected phytochemicals when interacting with ERa and ERb, with an emphasis on understanding the strength and characteristics of these interactions, which are crucial for explaining their potential therapeutic benefits.
- IV. To assess the potential inhibitory effects and therapeutic agents of the identified phytochemicals on pathways related to breast cancer, based on the findings from the molecular docking simulations.

Methodology

Screening and Preparation of Phytochemicals from chili leaves (*Capsicum frutescens*). Forty-nine main phytochemicals from the leaves of *Capsicum frutescens* (Batiha et al., 2020) were tested before docking. All 49 compounds underwent screening through Lipinski's rule of 5 to determine the drug-likeness of each compound through SwissADME (<http://www.swissadme.ch>), and to determine the toxicity through pkCSM (<https://biosig.lab.uq.edu.au/pkcsm/prediction>).

Lipinski's Rule of Five, formulated by Christopher A. Lipinski in 1997, states a set of guidelines used in drug discovery to predict whether a chemical compound is likely to be orally active in humans. These rules focus on the compound's physicochemical properties, suggesting that for a compound to be absorbed through the digestive system, it should meet specific criteria: it should have no more than five hydrogen bond donors (such as OH and NH groups) and no more than ten hydrogen bond acceptors (such as oxygen and nitrogen atoms), with a molecular weight of less than 500 daltons and a log P value (octanol-water partition coefficient) of less than 5, indicating its ability to dissolve in fats and lipids. While these rules provide a foundational framework for evaluating a compound's potential as a drug, there are exceptions, and some effective drugs may not adhere strictly to all the criteria. (Karami et al., 2022). The bioavailability, solubility, and chemical stability of each compound, as well as the likelihood of these molecules being replicated as drugs for use and commercial distribution, were all validated by this drug-likeness test.

Furthermore, pkCSM is a computational tool designed to predict the pharmacokinetic properties of small molecules, focusing on key ADMET characteristics. Utilizing graph-based signatures, it encodes the spatial relationships between atoms in a molecule, allowing for accurate predictions of absorption, distribution, metabolism, excretion, and toxicity. The tool is accessible as a free web server, enabling users to input molecular structures in SMILES format for rapid analysis. pkCSM has been validated across various classes of pharmacokinetic properties and performs comparably or better than existing methods. Its application in early-stage drug screening and structural optimization significantly enhances the drug discovery process by identifying compounds with favorable profiles early on (Pires et al., 2015).

Afterwards, only the compounds that were pkCSM and Lipinski test-passing were used in the Autodock Vina docking simulation. PyMOL was used to convert the SDF files to PDB format, and MGL AutodockTools and the Autodock Vina system were used to get the compounds ready for docking. The torsional degree of freedom and Gasteiger charges of each ligand were automatically set in AutodockTools via Autodock Vina. All compounds were saved as PDBQT files for docking after they had been optimized.

Preparation of Breast Cancer Cell Human Estrogen Receptor Alpha . The target protein's (3D) structure (RCSB PDB ID: 3ERT) and (RCSB PDB ID: 5TOA) was obtained as a 3D model from the RCSB Protein Data Bank (<https://www.rcsb.org/>) in PDB format. The PDB file was exported to MGL AutodockTools for preparation after being downloaded. Polar hydrogens and Kollman charges were added to the protein and dispersed equally after water molecules were eliminated (Sharma & Sharma, 2021). To be accessible by Autodock Vina, the altered protein file was saved as a PDBQT file.

Receptor Grid Box Manual Generation. The active binding residues of the 3ERT Human Estrogen Receptor alpha protein were predicted through CASTp (Tian et al., 2018). The receptor grid area was determined using Autodock Vina through MGL AutodockTools. The center of the grid box was positioned according to the active binding site in correspondence to the active residues of the main pocket of the receptor protein: MET 343, LEU 346, THR 347, LEU 349, ALA 350, ASP 351, GLU 353, LEU 354, GLU 380, TRP 383, LEU 384, LEU

387, MET 388, LEU 391, ARG 394, PHE 404, GLU 419, GLY 420, MET 421, ILE 424, LEU 428, GLY 521, MET 522, HIS 524, LEU 525, TYR 526, MET 528, LYS 529, CYS 530, VAL 533, VAL 534, PRO 535, LEU 536, TYR 537, LEU 539. The binding site size was minimized to 60x60x60 (Pratama et al., 2019) to lessen the probability of the software producing less accurate results and unnecessary binding outcomes. The XYZ values of the coordinates of the center of the grid box (x: 30.01; y: -1.913; z: 24.207), as well as the dimensions of the grid box (60x60x60) (Pratama et al., 2019), were written in a text document for the configuration file with the exhaustiveness level set to 8 and energy range of 3 as per default protocol (Fig 1.)

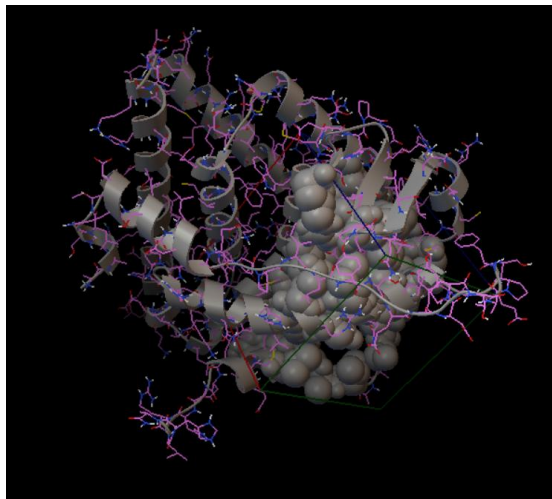


Fig 1. Estrogen Receptor Alpha (PDB ID:3ERT) receptor grid box visualization through MGL AutodockTools v. 1.5.7. Amino acids of the main binding site predicted by CastP were set to appear as spheres.

The active binding residues of the 5TOA Estrogen Receptor beta protein were predicted through CASTp (Tian et al., 2018). The receptor grid area was determined using Autodock Vina through MGL AutodockTools. The center of the grid box was positioned according to the active binding site in correspondence to the active residues of the main pocket of the receptor protein: ASP 326, ARG 329, GLU 332, SER 333, TRP 335, MET 336, GLU 337, MET 379, LEU 406, ASN 407, SER 408, SER 409, MET 410, TYR 411, SER 423, LEU 426, ALA 427, LEU 430, ASN 431, THR 434, ASP 435, VAL 438, ARG 466, HIS 467, SER 469, ASN 470, LYS 471, MET 473, GLU 474, LEU 477, ASN 478, CYS 481, TYR 488, ARG 329, GLU 332, SER 333, CYS 334, TRP 335, MET 336, GLU 337, MET 379, ALA 382, THR 383, ARG 386, GLU 389, LEU 390, SER 408, SER 409, MET 410, TYR 411, PRO 412, GLN 449, SER 452, MET 453, ALA 456, ASN 457, MET 460, LEU 461, HIS 464, ARG 466, HIS 467, ALA 468, SER 469, ASN 470, LYS 471, MET 473, GLU 474, LEU 477, ASN 478, CYS 481, TYR 488. The binding site size was minimized to 60x60x60 (Pratama et al., 2019) to lessen the probability of the software producing less accurate results and unnecessary binding outcomes. The XYZ values of the coordinates of the center of the grid box (x: 19.789; y: 43.343; z: 15.491), as well as the dimensions of the grid box (60x60x60) (Pratama et al., 2019), were written in a text document for the configuration file with the exhaustiveness level set to 8 and energy range of 3 as per default protocol (Fig 2.)

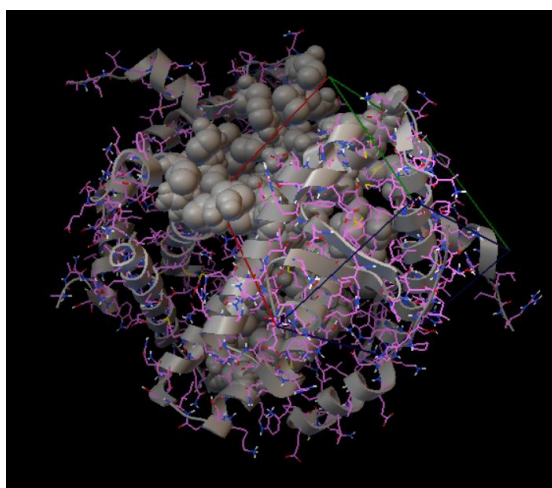


Fig 2. Estrogen Receptor Beta (PDB ID:5TOA) receptor grid box visualization through MGL AutodockTools v. 1.5.7. Amino acids of the main binding site predicted by CastP were set to appear as spheres.

Molecular Docking Analysis and Simulation. The docking analysis and simulation occurred after saving the optimized ligands, protein, and configuration files in the same folder. The Command Prompt on Windows 10 and 11 systems was used for the procedure. The computer's

Command Prompt was used to launch the Autodock Vina docking software. The location was changed to the directory of the folder containing the configuration files, ligand, and protein. Then the code:

```
C:\Program Files (x86)\The Scripps Research Institute\Vina\vina.exe" --receptor protein.pdbqt --ligand [ligand.pdbqt] --config [config.txt] --log [log.txt] --out [output.pdbqt]"
```

was written in the prompt for the computation (Forli et al., 2016; Trott & Olson, 2009). This docking was done, and the binding affinities of the molecules docked to the Human Estrogen Receptor Alpha (PDB ID: 3ERT) and Estrogen Receptor Beta (PDB ID: 5TOA) were given. This process was done ten times for each ligand. The text-formatted log files and the PDBQT-formatted simulation output files were the code's output files. Following the calculation, PyMol was used to import the protein files and output (in PDBQT format) for the 3D simulation. To visually depict the docking process between proteins and ligands, PyMOL, Chimera, and Ligplot+ were utilized.

Scoring and Analysis. The docking computation's output was stored in the same folder as the other docking files. The scoring and analysis of the docking results focused on the binding affinity between the ligands and the active site residues of Human Estrogen Receptor Alpha (PDB ID: 3ERT) and Estrogen Receptor Beta (PDB ID: 5TOA). In addition to measuring binding affinity—the degree of interaction between a ligand and a protein—a score function assesses the ligand's orientation and conformation within the protein's binding site. Binding affinity values were expressed in kcal/mol, a higher probability of successful binding is indicated by a more negative binding affinity score, which denotes a stronger interaction between the ligand and the protein (Forli et al., 2016; Wang et al., 2024). Results with the ligand inside the protein's main pocket were the only ones considered competent data. Considering that the compound is located inside the main pocket of the protein, the output with the lowest binding affinity value out of the five docking attempts was selected as the representative data for the docking interaction for each ligand. Protein-ligand interactions are stronger when the binding affinity value is lower because it signifies a higher energy release during binding, which creates a more stable complex between molecules and, consequently, a higher potential for protein-protein interaction inhibition (Ali et al., 2018; Seo et al., 2021). Values of -6 kcal/mol are typically regarded as acceptable for initial screening in drug design, whereas values of -7 kcal/mol or less are preferred for more thorough assessments. This indicates that the field is in agreement about the effectiveness of possible inhibitors (Ivanova & Karelson, 2022).

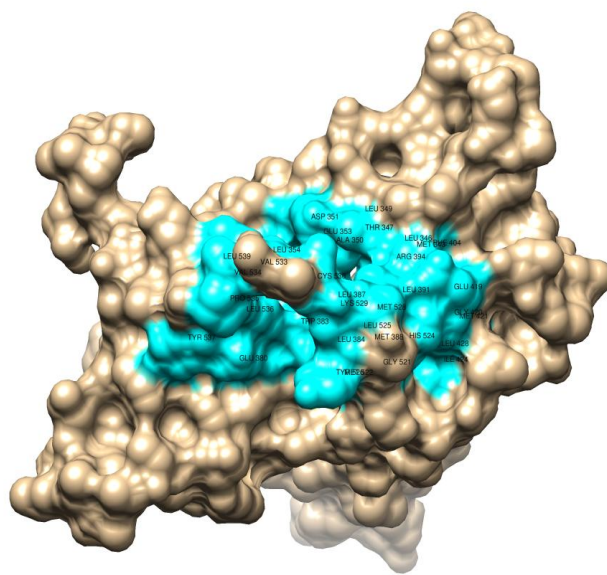


Fig 3. Interacting residues of ER α (PDB ID:3ERT)

Essential interacting residues in the Human Estrogen Receptor Alpha active sites have been examined, especially those related to hydrophobic and hydrogen bonding interactions. These residues included MET 343, LEU 346, THR 347, LEU 349, ALA 350, ASP 351, GLU 353, LEU 354, GLU 380, TRP 383, LEU 384, LEU 387, MET 388, LEU 391, ARG 394, PHE 404, GLU 419, GLY 420, MET 421, ILE 424, LEU 428, GLY 521, MET 522, HIS 524, LEU 525, TYR 526, MET 528, LYS 529, CYS 530, VAL 533, VAL 534, PRO 535, LEU 536, TYR 537, LEU 539. Furthermore, the amino acid residue of the protein-ligand interaction of 3ERT and 4-hydroxytamoxifen are also highlighted as it hints at possible biological activity, provides information on binding specificity and affinity, clarifies mechanisms of action, helps with drug design, and may affect the protein's stability and dynamics. These residues included MET 343, LEU 346, THR 347, ALA 350, ASP 351, GLU 353, TRP 383, LEU 387, ARG 394, MET 421, LEU 428, GLY 521 (Pratama et al., 2019).

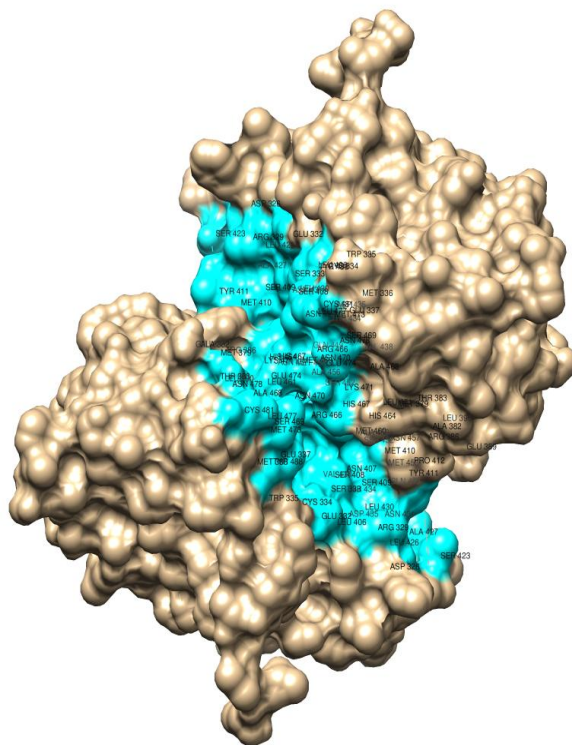


Fig 4. Interacting residues of ERβ (PDB ID:5TOA)

Essential interacting residues in the Human Estrogen Receptor Beta active sites have been examined, especially those related to hydrophobic and hydrogen bonding interactions. The binding sites for this protein are present in Chain A and Chain B. The residues in Chain A included ASP 326, ARG 329, GLU 332, SER 333, TRP 335, MET 336, GLU 337, MET 379, LEU 406, ASN 407, SER 408, SER 409, MET 410, TYR 411, SER 423, LEU 426, ALA 427, LEU 430, ASN 431, THR 434, ASP 435, VAL 438, ARG 466, HIS 467, SER 469, ASN 470, LYS 471, MET 473, GLU 474, LEU 477, ASN 478, CYS 481, and TYR 488. Whereas the residues in Chain B included ARG 329, GLU 332, SER 333, CYS 334, TRP 335, MET 336, GLU 337, MET 379, ALA 382, THR 383, ARG 386, GLU 389, LEU 390, SER 408, SER 409, MET 410, TYR 411, PRO 412, GLN 449, SER 452, MET 453, ALA 456, ASN 457, MET 460, LEU 461, HIS 464, ARG 466, HIS 467, ALA 468, SER 469, ASN 470, LYS 471, MET 473, GLU 474, LEU 477, ASN 478, CYS 481, and TYR 488.

Moreover, the amino acid residue of the protein-ligand interaction of 5TOA and Estradiol are also highlighted as it hints at possible biological activity, provides information on binding specificity and affinity, clarifies mechanisms of action, helps with drug design, and may affect the protein's stability and dynamics. These residues included GLU 305, MET 336, MET 340, LEU 343, ARG 346, PHE 356, ILE 376, LEU 380, GLY 472, and HIS 475 (Pratama et al., 2019).

A 3D depiction of each ligand's fit into the ERα and ERβ active sites was produced by using PyMOL to visualize the docking poses and interactions. 2D interaction maps were created using LigPlot+, emphasizing the particular hydrogen bonds and hydrophobic interactions that influenced the binding affinity. The binding of *Capsicum frutescens* phytochemicals to both 3ERT (estrogen receptor) and 5TOA, similar to interactions with 4-hydroxytamoxifen and estradiol, suggests the potential for modulating multiple biological pathways. This dual interaction indicates the possibility of multi-target therapeutic strategies, which could enhance treatment outcomes for complex diseases like cancer. Understanding these interactions provides valuable mechanistic insights into how these compounds influence receptor activity and their biological effects.

Methodological Framework

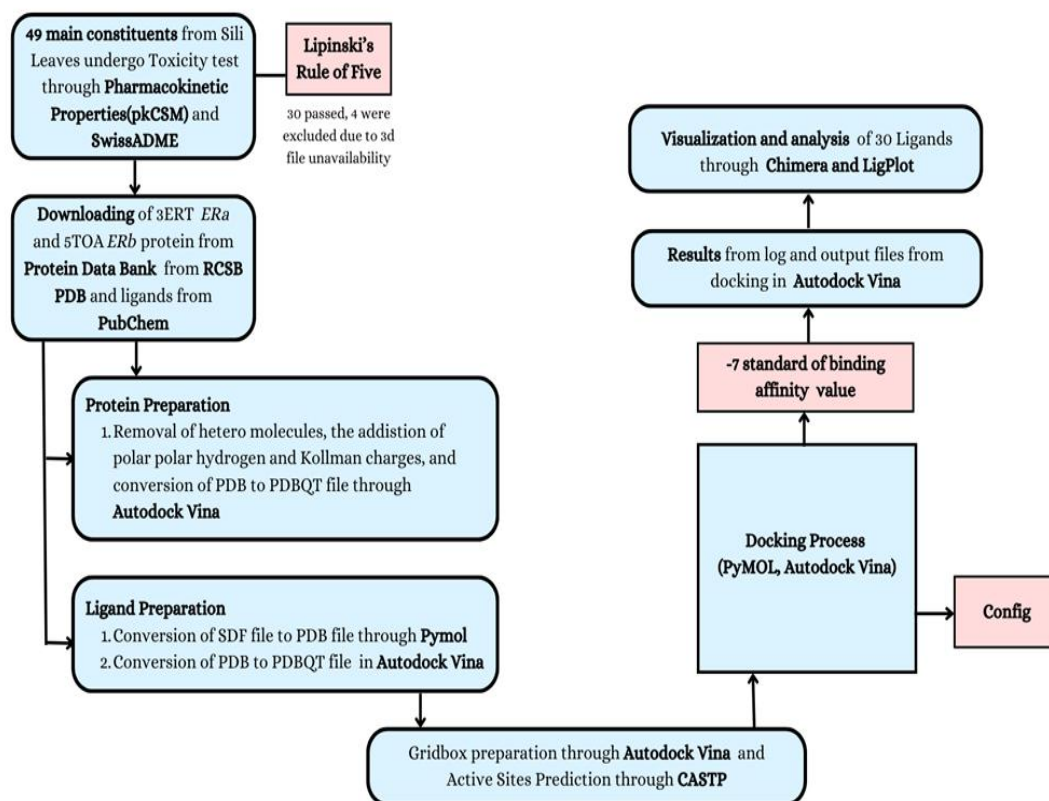


Fig 5. Methodological Framework of the Study

Results and Discussion

This study focused on identifying and analyzing 49 key phytochemical compounds derived from the leaves extract of *Capsicum frutescens*, targeting the active binding sites of the ERa and ERb proteins associated with breast cancer. These 49 phytochemicals were evaluated using SwissADME according to Lipinski's rule, where their physicochemical properties were assessed prior to molecular docking. Out of the 49 compounds, 30 met the criteria of Lipinski's rule of five and pkCSM toxicity.

Table 1: Phytochemicals found in *Capsicum Frutescens*

<i>a</i>	<i>b</i>	<i>c</i>	<i>d</i>	<i>e</i>	<i>f</i>
Sinapinic Acid	224.21	2	5	1.5	0
Nordihydrocapsiate	294.4	1	4	4.5	0
Cryptochlorogenic Acid	354.31	6	9	-0.4	1
Neochlorogenic Acid	354.31	6	9	-0.4	1
Glutamic Acid	147.13	3	5	-3.7	0
Aspartic Acid	133.10	3	5	-2.8	0

Caffeic acid	180.16	3	4	1.2	0
Chlorogenic acid	354.31	6	9	-0.4	1
Ferulic acid	224.21	2	5	1.5	0
Gallic acid	170.12	4	5	0.7	0
Vanillic acid	168.15	2	4	1.4	0
Cyanidin	287.24	5	5	0.5	0
Kaempferol	286.24	4	6	1.9	0
Myricetin	318.23	6	8	1.2	0
trans-p-sinapoyl glucopyranoside	d- 386.3	5	10	-1.1	0
Quercetin	448.4	7	11	0.9	0
Fructose	180.16	5	6	-2.8	0
Glucose	180.1	5	6	-2.6	0
Luteolin	286.24	4	6	1.4	0
Epicatechin	290.27	5	6	0.4	0
Catechin	290.27	5	6	0.4	0
Chrysoeriol	300.26	3	6	1.7	0
Apigenin	270.24	3	5	1.7	0
Capsiate	306.4	1	4	4.2	0
1-feruloyl-D-glucose.	356.32	5	9	-0.3	0
Dihydrocapsiate	308.4	1	4	5	0
Beta-Sitosterol	414.7	1	1	9.3	1
Stigmasterol	412.7	1	1	8.6	1
Limonene	136.23	0	0	3.4	0

Chitinase 395.5 1 7 2.2 0

a = Ligands; *b* = Molecular Weight (g/mol, <500 Da); *c* = Number of Hydrogen bond donors (<5); *d* = Number of Hydrogen bond acceptors (<10); *e* = M Log P_{ovv} (≤4.15); *f* = Number of Violations (<1)

In this study, 30 phytochemicals were docked with control variables on the 3ERT (Estrogen Receptor Alpha) and 5TOA (Estrogen Receptor Beta) protein from the PDB. To ensure accuracy and consistency, the docking process was repeated five times, to ensure both consistency and precision. Afterward, the docking procedure generated 5 different outputs with their corresponding reports. The output with the lowest binding affinity for each repetition was recorded.

Scoring Functions

PyMOL was employed to visualize and identify the positions of the five docking poses that occupied the protein's binding pocket. A standardized affinity value of -7 kcal/mol is used to highlight the phytochemicals with a higher probability of interacting with 3ERT and 5TOA. The standard binding affinity value is typically around -7.0 kcal/mol or lower when using tools like AutoDock Vina (Terefe & Ghosh, 2022). This process reduced the number of phytochemicals to 14 for PDB ID: 3ERT and 15 for PDB ID: 5TOA. The first pose of each ligand was saved in PDB files, and a total of 29 ligand complexes were subjected to visual analysis. Stigmasterol, Apigenin, and Cyanidin were found to have the most negative binding affinity scores in PDB ID: 3ERT. Cyanidin, Quercetin, Myricetin, Chinitase and Cryptochlorogenic Acid were found to have the most negative binding affinity scores in PDB ID: 5TOA.

Table 2: 14 Phytochemicals with -7.0 and Lower Binding Affinity Values in PDB ID: 3ERT

<i>a</i>	<i>b</i>	<i>c</i>	<i>d</i>
Cryptochlorogenic Acid	9798666	-7.3	Output 1
Neochlorogenic Acid	5280633	-7.2	Output 2
Chlorogenic acid	1794427	-7.2	Output 1
Cyanidin	128861	-7.8	Output 1
Kaempferol	5280863	-7.3	Output 1
Myricetin	5281672	-7.7	Output 1
Quercetin	5280459	-7.4	Output 1
Luteolin	5280445	-7.6	Output 1
Epicatechin	72276	-7.6	Output 1
Catechin	9064	-7.7	Output 1
Catechin	9064	-7.7	Output 1
Chrysoeriol	5280666	-7.4	Output 2
Apigenin	5280443	-8.0	Output 1
Stigmasterol	5280794	-8.7	Output 1

Chitinase	86223064	-7.1	Output 1
-----------	----------	------	----------

a = phytochemical name; *b* = CID from PUBCHEM (<5); *c* = binding affinity values; *d* = output number

Table 3: 26 Phytochemicals with -7.0 and Lower Binding Affinity Values in PDB ID: 5TOA

<i>a</i>	<i>b</i>	<i>c</i>	<i>d</i>
Cryptochlorogenic Acid	9798666	-8.1	Output 2
Neochlorogenic Acid	5280633	-7.9	Output 3
Dicaffeoylquinic Acid	6474310	-8.1	Output 3
Chlorogenic acid	1794427	-7.9	Output 4
Cyanidin	128861	-8.4	Output 3
Kaempferol	5280863	-7.8	Output 1
Myricetin	5281672	-8.1	Output 5
Quercetin	5280459	-8.2	Output 4
Luteolin	5280445	-7.8	Output 1
Epicatechin	72276	-7.9	Output 2
Catechin	9064	-7.8	Output 3
Chrysoeriol	5280666	-7.7	Output 5
Apigenin	5280443	-7.7	Output 2
Chrysoeriol	5280666	-7.4	Output 4

a = phytochemical name; *b* = CID from PUBCHEM (<5); *c* = binding affinity values; *d* = output number

Protein and Ligand Interactions between interacting residues

Breast cancer is a disease characterized by the uncontrolled growth of abnormal breast cells, leading to the formation of a tumor. It can cause severe symptoms, including large, painful lumps in the breast or armpit, skin changes, ulcers or sores on the breast, and nipple discharge or inversion. Estrogen Receptor Alpha (ER α), identified as PDB ID: 3ERT, and the Estrogen Receptor Beta PDB ID: 5TOA plays a crucial role in the cellular mechanism of cancer.

Molecular docking was employed to investigate the interactions between 30 phytochemicals that passed the Lipinski's Rule of Five and the active site of ER α and ER β . This research aims to determine how these compounds bind to the receptor's binding pocket. The findings revealed that 14 phytochemicals in their highest predicted conformations formed at least one interaction with key amino acid residues in the active binding site of 3ERT. Whereas, 15 phytochemicals, in their most stable forms, interacted with crucial residues in the binding pocket of 5TOA. All of these compounds demonstrated binding affinities of -7.0 kcal/mol or lower, suggesting strong potential for influencing the receptor's activity.

Table 4: Ligplot Analysis of the 14 Phytochemicals

<i>a</i>	<i>b</i>	<i>c</i>
Cryptochlorogenic Acid	LEU 525	LYS 529
	[3.00]	TYR 526
	CYS 530	MET 522
	[3.24]	
	GLU 523	
	[3.20]	
Neochlorogenic Acid	ASN 519	
	[2.96]	
	GLU 353	PHE 445
	[2.50]	GLY 390
	ARG 394	LYS 449
	[3.05]	TRP 393
	ILE 386	ILE 326
	[3.07]	GLU 329
		PRO 324
		LEU 327
	PRO 325	
Chlorogenic Acid	LEU 536	MET 522
	[3.14]	TYR 526
	LEU 525	
	[3.03]	
	GLU 523	
	[3.07]	
Cyanidin	ASN 519	
	[2.73]	
	GLU 353	GLU 323
	[2.94]	PRO 325
	ARG 394	ILE 326
	[3.07]	PRO 324
	GLY 390	LEU 387
	[3.05]	LYS 449
TRP 393		
	[3.01]	

Kaempferol	ARG 515	SER 512
	[3.33]	ASN 455
	THR 483	LEU 511
	[3.14]	ILE 451
		LEU 508
		LEU 479
Myricetin	TRP 393	GLU 323
	[3.20]	PRO 324
	ARG 394	ILE 326
	[3.08]	GLY 390
	ILE 386	GLU 353
	[3.14]	LEU 387
	PRO 325	LYS 449
	[3.15]	
Quercetin	GLU 353	ILE 326
	[2.96]	GLU 323
	ARG 394	PRO 325
	[3.06]	GLY 390
	TRP 393	PRO 324
	[3.13]	LEU 387
		LYS 449
Luteolin	GLU 353	MET 357
	[3.21]	ILE 386
		LEU 387
		PRO 324
		GLY 390
		ILE 326
		ARG 394
		LYS 449
		TRP 393
		GLU 323
		PRO 325
		HIS 356
	Epicatechin	TRP 393
[3.03]		ARG 394

	GLU 353	GLU 323
	[3.02]	PRO 324
		MET 357
		LYS 449
		GLY 390
		LEU 387
		ILE 386

Catechin	GLU 353	ILE 326
	[3.09]	GLU 323
	GLY 390	PRO 324
	[2.91]	PRO 325
	ARG 394	LYS 449
	[2.96]	LEU 387
	TRP 393	
	[3.10]	

Chrysoeriol	GLU 353	LEU 387
	[3.21]	ILE 386
		MET 357
		GLY 390
		LYS 449
		TRP 393
		ILE 326
		GLU 323
		PRO 324
		PRO 325
		HIS 356

Apigenin	GLU 353	MET 357
	[3.19]	HIS 356
		ILE 386
		LEU 387
		PRO 324
		PRO 325
		GLY 390
		GLU 323
		LYS 449
		TRP 393

		ARG 394
		ILE 326
Stigmasterol	N/A	ARG 515
		SER 512
		ILE 451
		LEU 511
		ASN 455
		ARN 546
		THR 483
		LEU 479
		LEU 508
		ASP 480
Chitinase	TRP 393	GLY 390
	[3.21]	PRO 325
		GLU 353
		ILE 326
		PRO 324
		ARG 394
		GLU 323
		LEU 320
		ASP 321

a = phytochemical name; *b* = hydrogen bonds with interacting residues; *c* = Hydrophobic interactions with interacting residues; **bold** = binding sites

Apigenin, Cyanidin, Myricetin, and Catechin are the leading ligands according to this ranking. The ligands exhibited a diverse array of remarkable binding affinities, wherein Apigenin exhibited the second highest value of -8.0 kcal/mol, followed by Cyanidin at -7.8 kcal/mol, then a tie of Myricetin and Catechin at -7.7 kcal/mol.

The consistent outcomes underscore the potency of the compounds' binding and their specific interaction with critical residues. The insights provided by this data are of great value in advancing the investigation of these ligands as possible inhibitors, thereby enhancing our comprehension of their therapeutic capabilities in relation to viral infections. The assessment of each compound's inhibitory potential hinged upon evaluating their respective binding affinity levels and the involvement of interactive residues, encompassing hydrogen bonds and hydrophobic interactions among molecules. Binding affinity within molecular docking denotes the robustness of the interaction occurring at a specific binding site between a ligand and a receptor, foretelling the probability and strength of their association. Notably, the substantial contributions of hydrogen bonds and hydrophobic interactions between molecules significantly impact the efficacy of the phytochemicals from *Capsicum Frutescens* binding to the Estrogen Receptor Alpha (ERα) protein.

Apigenin demonstrated interaction with three pivotal binding sites on the ERα to 4-hydroxytamoxifen—specifically, GLU 353, LEU 387, and ARG 394—engaging the GLU 353 at a distance of 3.19 Å in hydrogen bonds and the LEU 387 and ARG 394 in hydrophobic interactions. It interacted with three prominent amino acids from ERα within the 12 critical residues of 3ERT to 4-hydroxytamoxifen receptors.

Table 5: Ligplot Analysis of the 15 Phytochemicals

<i>a</i>	<i>b</i>	<i>c</i>
----------	----------	----------

Cryptochlorogenic Acid	LYS401	MET309
	[2.81]	PRE277
	TY397	TRP345
	[2.77]	ARG346
	GLU305	HIS279
	[2.74, 2.73, 2.65]	LEU339 HIS308
Neochlorogenic Acid	LYS401	VAL280
	[3.11]	GLY342
	TYR397	PRO277
	[3.14, 2.66]	TRP345
	GLU276	PRO278
	[2.70]	GLU305
	ARG346	
	[2.91]	
	HIS279	
	[3.20]	
Dicafeoylquinic Acid	SER333	EHE325
	[3.15, 2.93]	ARG329
	MET410	SER409
	[3.03]	GLU332
	SER408	TYR448
	[3.14, 3.16]	MET437
	ASP489	VAL328
	[2.31]	
	TRP335	
	[3.01]	
	HIS467	
[3.02]		
Chlorogenic acid	VAL338	GLY342
	[2.98]	LEU339
	LYS401	TYR397
	[3.07]	GLU376
	TRP345	BIS399
	[3.03]	PRO377
	HIS394	

	[3.03, 3.21]	
	PRO278	
	[3.12]	
	GLU305	
	[2.71, 3.23]	
	ARG346	
	[2.30]	
Cyanidin	ASN407	LEU406
	[2.92]	HIS464
	TYR411	MET410
	[2.96]	ARG386
		GLU389
		SER385
		LEU426
		SER409
		ALA427
		LEU430
Kaempferol	ARG329	HIS464
	[3.09]	SER409
	ARG386	MET410
	[3.33]	LEU430
	ASN431	LEU426
	[3.24, 3.00]	ALA427
	SER423	LEU430
	[3.17]	
Myricetin	TRP345	TYR397
	[3.24]	PRO227
	GLU276	LEU339
	[2.97]	MET309
	VAL338	HIS279
	[3.07]	ARG246
	GLU305	HIS308
	[3.00, 2.76, 3.25]	
Quercetin	ASN357	ARG386

	[3.00]	LEU426
	SER409	LEU430
	[3.18, 2.90]	ASN407
	LEU406	HIS464
	[2.88]	
	ASN431	
	[2.88]	
Luteolin	ARG386	TYR411
	[3.11]	MET410
	ASN431	HIS464
	[2.71, 3.02]	SER409
	ASN457	LEU426
	[2.71, 3.17]	LEU430
		ALA427
Epicatechin	ARG329	TYR411
	[3.83]	MET410
	ARG386	LEU426
	[3.05]	SER409
	ASN	HIS464
	[3.51, 3.36]	LEU430
	ASN431	ALA427
	[3.51]	
Catechin	GLU305	HIS308
	[3.19]	ARG346
	PRO227	GLU276
	[2.89]	TRP345
	PRO278	TYR397
	[2.98]	LRU339
	HIS279	MET309
	[3.13]	
	VAL338	
	[2.91]	
Chrysoeriol	TYR397[2.99]	GLY342
	LYS401	GLU276
	[3.00]	HIS279

	TRP345	ARG316
	[3.05]	VAL280
	PRO278	GLU305
	[3.07]	PRO277
Apigenin	GLU305	TYR397
	[2.94]	GLU276
		TRP345
		ARG346
		GLY342
		LYS401
		MET389
		LEU339
		PRE227
		HIS279
1-feruloyl-D-glucose.	GLU276	VAL 280
	[3.13]	ARG 346
	LYS 401	PRO 277
	[3.06]	TRP 345
	TYR397	ILE 348
	[2.98]	
	HIS279	
	3.21	
	GLU305	
	[3.29, 2.71]	
Chitinase	ASN431	HIS428
	[3.20]	LEU430
	ASN431	ARG386
	[2.97]	GLU389
		ALA427
		ARG424

a = phytochemical name; *b* = hydrogen bonds with interacting residues; *c* = Hydrophobic interactions with interacting residues; **bold** = binding sites

Cyanidin, Quercetin, and Cryptochlorogenic Acid were identified as the top ligands based on binding affinity rankings. Cyanidin exhibited the highest binding affinity at -8.4 kcal/mol, followed closely by Quercetin with -8.2 kcal/mol, and Cryptochlorogenic Acid and Dicafeoylquinic Acid both at -8.1 kcal/mol. These results prove that these ligands have a promising capacity to interact with the target protein.

The consistent results highlight the strength of the ligands' binding capabilities and their precise interactions with key residues. This data is highly valuable in advancing the study of these compounds as potential inhibitors, broadening this research understanding of their therapeutic potential in the field of breast cancer. Each compound's inhibitory potential was assessed by examining their binding affinity levels and the involvement of interactive residues, which included both hydrogen bonds and hydrophobic contacts. In molecular docking, binding affinity measures the strength of the interaction between a ligand and a receptor at a specific binding site, predicting both the likelihood and strength of their association. Hydrogen bonds and hydrophobic interactions play a crucial role in stabilizing these molecular connections, significantly influencing the efficacy of the phytochemicals from *Capsicum Frutescens* interaction with the Estrogen Receptor Beta (ER β) protein.

Cyanidin was observed to engage with several crucial residues in the 5TOA protein, forming both hydrogen bonds and hydrophobic interactions that significantly contributed to its stability within the binding pocket. Among the 71 residues present in the 5TOA structure, Cyanidin formed hydrogen bonds with key sites while also establishing hydrophobic contacts with multiple residues, demonstrating a strong affinity for the receptor. The binding affinity of Cyanidin was recorded at -8.4 kcal/mol, highlighting its potential as a stable and effective ligand. The combination of hydrogen bonds and hydrophobic interactions enhances the strength of this interaction, underscoring the important role of these forces in maintaining docking stability. These results indicate that Cyanidin has significant potential for interaction with the 5TOA protein.

Top Two Phytochemicals with the most interacting residues of 3ERT

Apigenin demonstrated interaction with three pivotal binding sites on the ER α to 4-hydroxytamoxifen—specifically, GLU 353, LEU 387, and ARG 394—engaging the GLU 353 at a distance of 3.19 Å in hydrogen bonds and the LEU 387 and ARG 394 in hydrophobic interactions. It interacted with three prominent amino acids from ER α within the 12 critical residues of 3ERT to 4-hydroxytamoxifen receptors. Apigenin holds the second most leading binding affinity at -8.0 kcal/mol.

Cyanidin exhibits strong binding interactions with the target site of 3ERT, demonstrating a binding affinity of -7.8 kcal/mol, positioning it as the third most potent compound. This compound forms six hydrophobic interaction residues with one pivotal residue matched on the 12 critical residues on ER α to 4-hydroxytamoxifen—notably LEU 387, which directly contributes to its stability at the binding site. Additionally, Cyanidin forms hydrogen bonds with two crucial residues GLU 353 and ARG 394 at distances of 2.94 Å, 3.07 Å respectively, emphasizing its effectiveness.

Top Three Phytochemicals with the most interacting residues of 5TOA

Cyanidin was found to interact with ten key residues on the 5TOA protein, highlighting its binding capability. Among 71 residues of the 5TOA, it formed two hydrogen bonds with ASN 407 measured at distance of 2.92 Å and TYR 411 at a distance of 2.96 Å and , while engaging in eight hydrophobic interactions with LEU 406, HIS 464, MET 410, ARG 386, GLU 389, LEU 426, SER 409, and ALA 427. This combination of hydrogen bonds and hydrophobic contacts indicates a strong affinity for the protein, with a binding affinity measured at -8.4 kcal/mol. These findings suggest that Cyanidin holds promising potential as an effective ligand for 5TOA protein

Quercetin is the second to have the most interacting residues having 8 pivotal residues on the 5TOA protein, forming multiple hydrophobic interactions and hydrogen bonds that enhance its binding stability. Key residues include 3 hydrogen bonds which are SER409 measured at distances of 3.18 Å and 2.90 Å, LEU406 measured at distances of 2.88 Å and ASN431 measured at a distance of 2.88 Å, engaging with 5 hydrophobic interactions with ARG386, LEU426, LEU430, ASN407, HIS46 BN4 providing its strong binding capacity. With a calculated binding affinity of -8.2 kcal/mol, Quercetin is positioned as a potent compound within the study. These findings suggest that Luteolin has significant potential as an inhibitor of the 5TOA protein.

Dicaffeoylquinic Acid was found to interact with 8 essential residues on the 5TOA protein, making it as the third most potent compound forming strong hydrophobic interactions that contribute to its stability at the binding site. Key residues involved include SER333, MET410, SER408 TRP335, and HIS467. Dicaffeoylquinic Acid formed 5 hydrogen bonds with SER333 at a distance of 3.15 Å 2.93 Å , MET410 measured at distance of 3.03 Å, SER408 at a distance of 3.14 Å and 3.16 Å, TRP335 at a distance of 3.01 Å and HIS467 at a distance of 3.02Å. It also engages with 3 hydrophobic interactions with ARG329, SER409, and GLU332 further solidifying its interaction strength. With a binding affinity measured at -8.1 kcal/mol, Dicaffeoylquinic Acid is recognized as a strong candidate among the compounds studied. These interactions highlight Dicaffeoylquinic Acid's potential as an effective inhibitor of the 5TOA protein.

Other Phytochemicals with notable interacting residues of 3ERT

Exhibiting a collective binding affinity level of -7.7 kcal/mol, Myricetin is the fourth most potent compound regarding binding affinity among all the compounds tested. It has a high potential for NiVG inhibition. Three of the crucial binding sites of ER α to the 4-hydroxytamoxifen host cell receptor are determined, fostering one crucial amino acid of hydrogen bond—specifically, ARG 394 at a distance of 3.08 Å, and a hydrophobic interaction with GLU 353 and LEU 387 key residues in the 4-hydroxytamoxifen binding to the Estrogen Receptor Alpha.

Catechin interacted with key ER α binding sites—GLU 353, ARG 394, and LEU 387 essential 4-hydroxytamoxifen receptor-binding residues. Moderate hydrogen bonding (3.09 Å and 2.96 Å) with GLU 353 and ARG 394 and hydrophobic contact with LEU 387 displayed a

binding affinity of -7.7 kcal/mol as well. Catechin enhanced binding affinity by forming hydrogen bonds with ERa residues in 4-hydroxytamoxifen receptor contacts. These hydrogen bonds contribute to the ligand's specificity for receptor binding, while concurrent hydrophobic interactions bolster its overall stability. Catechin may inhibit ERa due to its hydrogen bonds and hydrophobic interactions.

Luteolin displayed a binding affinity of -7.6 kcal/mol, engaging with two critical binding sites—LEU 387 and ARG 394—via 12 hydrophobic interactions. It also formed a hydrogen bond with GLU 353 at a distance of 3.21 Å, directly interacting on 3ERT to 4-hydroxytamoxifen residues.

Epicatechin demonstrated a similar -7.6 kcal/mol affinity, forming 9 hydrophobic interactions with its crucial residues—specifically ARG 394 and LEU 387 on 3ERT to 4-hydroxytamoxifen. Additionally, it established hydrogen bonds with TRP 393 at 3.03 Å and GLU 353 at 3.02 Å, with GLU 353 serving as the direct interaction with 3ERT to 4-hydroxytamoxifen

The 8 remaining ligands were Stigmasterol, Neochlorogenic Acid, Chlorogenic acid, Cryptochlorogenic Acid, Kaempferol, Quercetin, Chrysoeriol, and Chitinase with their respective binding affinities -8.7 kcal/mol, -7.2 kcal/mol, -7.2 kcal/mol, -7.3 kcal/mol, -7.3 kcal/mol, -7.4 kcal/mol, -7.4 kcal/mol, -7.1 kcal/mol.

Other Phytochemicals with notable interacting residues of 5TOA

The results of the molecular docking study highlight the interactions between various phytochemicals and the 5TOA protein, offering insight into their potential as inhibitors based on binding affinities and interactions with key residues. Out of all the compounds tested, Cryptochlorogenic Acid and Myricetin showed the highest binding affinity at -8.1 kcal/mol, with neither forming hydrogen bonds and significant hydrophobic interactions. These findings suggest that, despite the absence of hydrogen bonds and hydrophobic interactions, they are still crucial in stabilizing these compounds within the binding pocket since they have a low binding affinity. Neither formed hydrogen bonds, and hydrophobic interactions with key residues, but they are still highlighted for their potential in stable receptor binding.

Neochlorogenic Acid and Chlorogenic Acid followed with binding affinities of -7.9 kcal/mol. Similarly, these compounds did not form hydrogen bonds and hydrophobic interactions, but they are still crucial for stabilizing their interactions with the protein target.

Kaempferol, with a binding affinity of -7.8 kcal/mol, formed four hydrogen bonds with ARG329 with a distance of 3.09 Å, ARG386 with a distance of 3.33 Å, ASN431 with a distance of 3.24 Å and 3.00 Å, and SER423 at a distance of 3.17 Å. In addition, it engaged in hydrophobic interactions with HIS464, SER409, MET410, LEU426, and ALA427. These interactions contribute to Kaempferol's binding stability and potential therapeutic relevance.

Luteolin, which exhibited a binding affinity of -7.8 kcal/mol, formed three hydrogen bonds with ARG386 at a distance of 3.83 Å, ASN431 at a distance of 2.71 Å and 3.02 Å, and ASN457 at distances of 2.71 Å and 3.17 Å. It also showed extensive hydrophobic interactions with residues such as TYR411, MET410, LEU426, SER409, HIS464, LEU430, and ALA427 reinforcing its binding potential and stability at the receptor.

Epicatechin, with a binding affinity of -7.9 kcal/mol, established three hydrogen bonds with ARG329 at a distance of 3.83 Å, ARG386 at a distance of 3.05 Å, and ASN431 at a distance of 3.51 Å, alongside multiple hydrophobic interactions with residues TYR411, MET410, LEU426, SER409, HIS464, LEU430, and ALA427. These interactions suggest a strong binding capability for Epicatechin, contributing to its therapeutic potential.

Catechin, with a binding affinity of -7.8 kcal/mol, did not exhibit any hydrogen bonds or hydrophobic interactions. However, its high negative binding affinity indicates it still has a role in stabilizing its interaction with the target, highlighting its potential relevance.

Chrysoeriol and Apigenin, both with binding affinities of -7.7 kcal/mol, neither formed hydrogen bonds nor engaged in hydrophobic interactions with the receptor. Despite this, their binding affinities suggest potential as they may interact through other mechanisms, making them worthy of further investigation.

Similarly, 1-Feruloyl-D-glucose, despite not forming hydrogen bonds and lacking hydrophobic interactions, demonstrated a binding affinity of -7.5 kcal/mol. This suggests that other interaction mechanisms may contribute to its relevance in ligand-receptor binding.

Chitinase, with a strong binding affinity of -8.1 kcal/mol, formed two hydrogen bonds with ASN431 at distances of 3.20 Å and ASN430 both at a distance of 2.97 Å, along with hydrophobic interactions with residues LEU430, ARG386, GLU389 and ALA427. These interactions reinforce its position as a potent compound for further exploration in receptor binding studies.

Visualization of the top two Phytochemicals with the most interacting residues of 3ERT

Apigenin

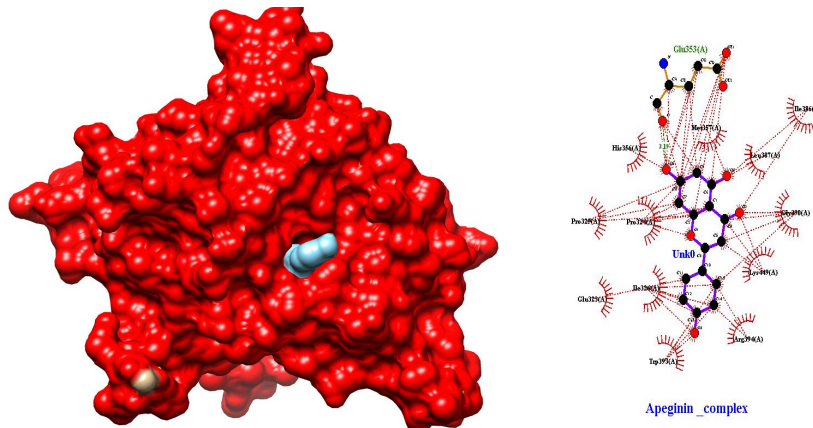


Figure 6. Apeginin-3ERT complex. Chimera 3D visualization (left); Ligplot + hydrogen bonds and hydrophobic interactions 2D visualization (right).

Cyanidin

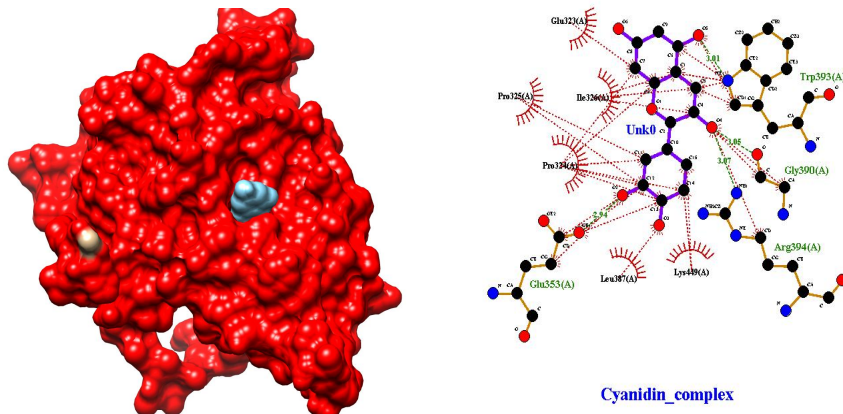


Figure 7. Cyanidin-3ERT complex. Chimera 3D visualization (left); Ligplot + hydrogen bonds and hydrophobic interactions 2D visualization (right).

Visualization of the top three Phytochemicals with the most interacting residues of 5TOA

Cyanidin

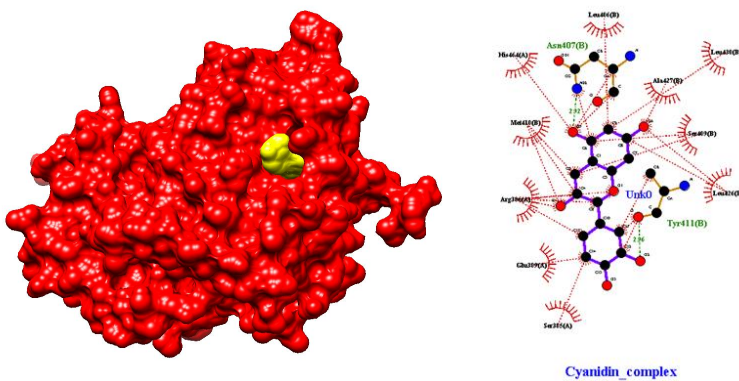


Figure 8. Cyanidin-5TOA complex. Chimera 3D visualization (left); Ligplot + hydrogen bonds and hydrophobic interactions 2D visualization (right).

Quercetin

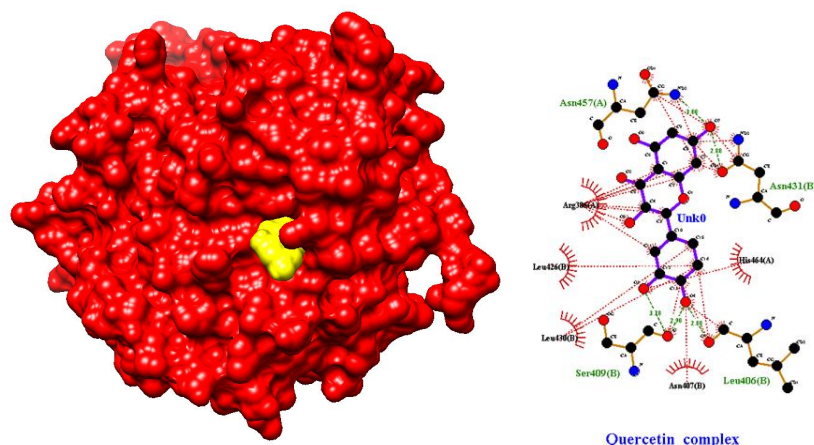


Figure9. Quercetin-5TOA complex. Chimera 3D visualization (left); Ligplot + hydrogen bonds and hydrophobic interactions 2D visualization (right).

Dicaffeoylquinic Acid

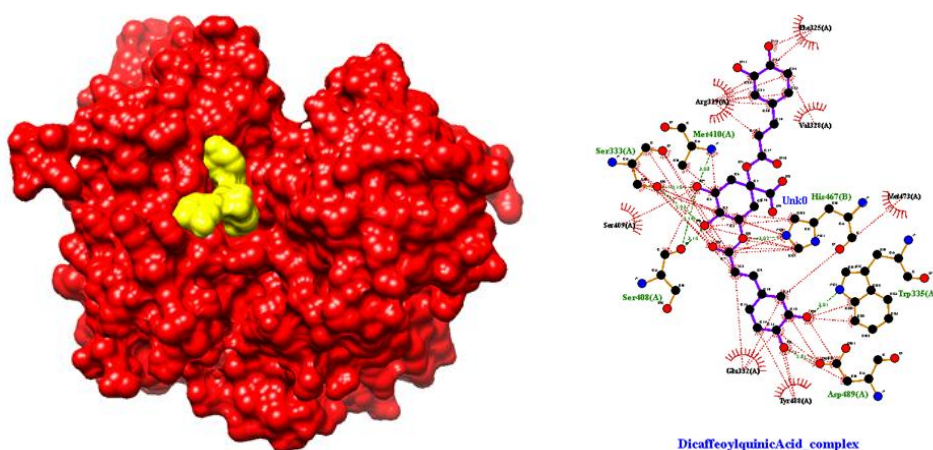


Figure 10 . Dicaffeoylquinic Acid-5TOA complex. Chimera 3D visualization (left); Ligplot + hydrogen bonds and hydrophobic interactions 2D visualization (right).

Conclusions and Recommendations

The in silico docking analysis of chili leaves (*Capsicum frutescens*) revealed promising phytochemicals that may inhibit breast cancer-related proteins. Stigmasterol showed the strongest binding affinity to Estrogen Receptor Alpha (ER α), while Cyanidin exhibited potential against Estrogen Receptor Beta (ER β). These findings suggest that these compounds could serve as inhibitors, but further validation is needed through biological testing.

To confirm their therapeutic potential, in vitro studies on breast cancer cell lines should be conducted. This will help assess how effectively these compounds inhibit cancer cell growth in a real biological environment. Additionally, applying Quantitative Structure-Activity Relationship (QSAR) modeling will aid in predicting the biological activity of these compounds based on their molecular structures, refining the selection of the most promising candidates.

Future research should also explore dose-response studies to identify safe and effective concentrations of these phytochemicals. Biochemical assays and molecular dynamics simulations can further elucidate their interactions with target proteins, providing deeper insights into their mechanisms.

In conclusion, while the in silico and QSAR analysis suggest that *Capsicum frutescens* phytochemicals could potentially treat breast cancer, these results require validation through in vitro and in vivo testing. A combination of computational and laboratory methods will help determine their true therapeutic potential.

Acknowledgments

The researchers would like to extend their heartfelt gratitude to Sir Sherwin Fortugaliza for his support and encouragement. The researchers would like to acknowledge him for providing important thoughts that have contributed a lot to their research and kept the researchers motivated. Moreover, the researcher's families and friends are acknowledged for their unwavering support, encouragement, and understanding during the research journey, especially their family who provided for them for their research, serving as their continual source of inspiration. Lastly, the researchers would very much like to acknowledge and give thanks to God for providing the strength, wisdom, and guidance they needed to overcome the challenges and have successful research.

References:

- Agu, P. C., Afiukwa, C. A., Orji, O. U., Ezeh, E. M., Ofoke, I. H., Ogbu, C. O., Ugwuja, E. I., & Aja, P. M. (2023). Molecular docking as a tool for the discovery of molecular targets of nutraceuticals in disease management. *Scientific Reports*, 13(1). <https://doi.org/10.1038/s41598-023-40160-2>
- Akhtar, A., Asghar, W., & Khalid, N. (2021). Phytochemical constituents and biological properties of domesticated capsicum species: a review. *Bioactive Compounds in Health and Disease - Online ISSN 2574-0334 Print ISSN 2769-2426*, 4(9), 201. <https://doi.org/10.31989/bchd.v4i9.837>
- Al-Ostoot, F., Hezam, S., Khamees, S., Hussien, A., & Khanum, S. (2021). Tumor angiogenesis: Current challenges and therapeutic opportunities. *Journal of Cancer Research and Clinical Oncology*, 147(4), 895-908. <https://doi.org/10.1007/s00432-020-03468-9>
- Arnarson, A. (2023). Chili Peppers 101: Nutrition Facts and Health Effects. <https://www.healthline.com/nutrition/foods/chili-peppers>
- Asiamah, I., Obiri, S. A., Tamekloe, W., Armah, F. A., & Borquaye, L. S. (2023). Applications of molecular docking in natural products-based drug discovery. *Scientific African*, 20, e01593. <https://doi.org/10.1016/j.sciaf.2023.e01593>
- Batiha, G. E., Alqahtani, A., Ojo, O. A., Shaheen, H. M., Wasef, L., Elzeiny, M., Ismail, M., Shalaby, M., Murata, T., Zaragoza-Bastida, A., Rivero-Perez, N., Beshbishy, A. M., Kasozi, K. I., Jeandet, P., & Hetta, H. F. (2020). Biological Properties, Bioactive Constituents, and Pharmacokinetics of Some Capsicum spp. and Capsaicinoids. *International Journal of Molecular Sciences*, 21(15), 5179. <https://doi.org/10.3390/ijms21155179>
- Bender, B. J., Gahbauer, S., Luttens, A., Lyu, J., Webb, C. M., Stein, R. M., Fink, E. A., Balius, T. E., Carlsson, J., Irwin, J. J., & Shoichet, B. K. (2021). A practical guide to large-scale docking. *Nature Protocols*, 16(10), 4799–4832. <https://doi.org/10.1038/s41596-021-00597-z>
- Breast cancer*. (2024, September 9). *Cleveland Clinic*. <https://my.clevelandclinic.org/health/diseases/3986-breast-cancer>
- Breast cancer - Symptoms and causes*. (n.d.). Mayo Clinic. <https://www.mayoclinic.org/diseases-conditions/breast-cancer/symptoms-causes/syc-20352470>
- Capsicum frutescens (Sili) – Herbanext Laboratories, Inc.* (n.d.). <https://www.herbanext.com/medicinal-herbs/capsicum-frutescens-sili>
- Cleveland Clinic (n.d.). CAR-T Cell Therapy. Retrieved from <https://my.clevelandclinic.org/health/treatments/17726-car-t-cell-therapy>
- Co, L. M. B., Dee, E. C., Eala, M. a. B., Ang, S. D., & Ang, C. D. U. (2022). Access to surgical treatment for breast cancer in the Philippines. *Annals of Surgical Oncology*, 29(11), 6729–6730. <https://doi.org/10.1245/s10434-022-12311-8>
- Cortes-Ferre, H. E., Antunes-Ricardo, M., & Gutiérrez-Urbe, J. A. (2022). Enzyme-assisted extraction of anti-inflammatory compounds from habanero chili pepper (*Capsicum chinense*) seeds. *Frontiers in Nutrition*, 9. <https://doi.org/10.3389/fnut.2022.942805>
- Eberhardt, J., Santos-Martins, D., Tillack, A. F., & Forli, S. (2021). AutoDock Vina 1.2.0: new docking methods, expanded force field, and Python bindings. *Journal of Chemical Information and Modeling*, 61(8), 3891–3898. <https://doi.org/10.1021/acs.jcim.1c00203>
- Faiza, M. (2022). PyMol Uses and Applications. Retrieved from <https://bioinformaticsreview.com/20220202/pymol-uses-applications/>
- Feng, T., Wan, Y., Dai, B., & Liu, Y. (2023a). Anticancer Activity of Bitter Melon-Derived Vesicles Extract against Breast Cancer. *Cells*, 12(6), 824. <https://doi.org/10.3390/cells12060824>
- Ferlay J, Ervik M, Lam F, Laversanne M, Colombet M, Mery L, et al. "GLOBOCAN 2020: Global Cancer Observatory." International Agency for Research on Cancer. 2020. Available at: [GLOBOCAN 2020 - Philippines Fact Sheet](https://gco.iarc.fr/today/data/dataviz/globocan-2020-philippines) .
- Fernandez, R. a. T., & Ting, F. I. L. (2023). Achieving health equity in cancer care in the Philippines. *Ecancermedicalscience*, 17. <https://doi.org/10.3332/ecancer.2023.1547>
- Forli, S., Huey, R., Pique, M. E., Sanner, M. F., Goodsell, D. S., & Olson, A. J. (2016a). Computational protein–ligand docking and virtual drug screening with the AutoDock suite. *Nature Protocols*, 11(5), 905–919. <https://doi.org/10.1038/nprot.2016.051>

- Hope From Within. (2020, June 19). What to do after you find a lump in your breast, and more: The Breast Cancer Map. <https://hopefromwithin.org/what-to-do-after-you-find-a-lump-in-your-breast-and-more-the-breast-cancer-map/>
- Ivanova, L., & Karelson, M. (2022). The Impact of Software Used and the Type of Target Protein on Molecular Docking Accuracy. *Molecules*, 27(24), 9041. <https://doi.org/10.3390/molecules27249041>
- Jang, H., Choi, M., & Jang, K. (2024). Comprehensive phytochemical profiles and antioxidant activity of Korean local cultivars of red chili pepper (*Capsicum annuum* L.). *Frontiers in Plant Science*, 15. <https://doi.org/10.3389/fpls.2024.1333035>
- Karami, T. K., Hailu, S., Feng, S., Graham, R., & Gukasyan, H. J. (2021). Eyes on Lipinski's Rule of Five: a new "Rule of Thumb" for physicochemical design space of ophthalmic drugs. *Journal of Ocular Pharmacology and Therapeutics*, 38(1), 43–55. <https://doi.org/10.1089/jop.2021.0069>
- Kennedy, D. C., Coen, B., Wheatley, A. M., & McCullagh, K. J. A. (2021). Microvascular Experimentation in the Chick Chorioallantoic Membrane as a Model for Screening Angiogenic Agents including from Gene-Modified Cells. *International Journal of Molecular Sciences*, 23(1), 452. <https://doi.org/10.3390/ijms23010452>
- Kooti, W., Servatyari, K., Behzadifar, M., Asadi-Samani, M., Sadeghi, F., Nouri, B., & Marzouni, H. Z. (2017). Effective Medicinal Plant in Cancer Treatment, Part 2: Review study. *Journal of Evidence-Based Complementary & Alternative Medicine*, 22(4), 982–995. <https://doi.org/10.1177/2156587217696927>
- Kristine, E. (2023, September 29). *What are Chili Leaves? And 8 Best Alternatives!* The Kitchen Abroad. <https://www.thekitchenabroad.com/what-are-chili-leaves/>
- Kurman, Y., Kilicciglu, I., Dikmen, A. U., Esendagli, G., Bilen, C. Y., Sozen, S., & Konac, E. (2020). Cucurbitacin B and cisplatin induce the cell death pathways in MB49 mouse bladder cancer model. *Experimental Biology and Medicine*, 245(9), 805–814. <https://doi.org/10.1177/1535370220917367>
- Lee, S., & Min, K. (2019). *Drosophila melanogaster* as a model system in the study of pharmacological interventions in aging. *Translational Medicine of Aging*, 3, 98–103. <https://doi.org/10.1016/j.tma.2019.09.004>
- Lopes-Coelho, F., Martins, F., & Pereira, S. A. (2021). Anti-Angiogenic Therapy: Current Challenges and Future Perspectives. "Frontiers in Molecular Medicine", 1, 749283. <https://doi.org/10.3389/fmmed.2021.749283>
- Malvern Panalytical. (n.d.). *Binding affinity*. <https://www.malvernpanalytical.com/en/products/measurement-type/binding-affinity#~:~:text=Understanding%20binding%20affinity%20is%20key,their%20targets%20selectively%20and%20specifically>
- Martins, F., Lopes-Coelho, F., & Pereira, S. A. (2023). The Role of Angiogenesis Inhibition in Cancer Treatment: A Review. "Cancer Treatment Reviews", 115, 102203.
- Mecca, M., Sichetti, M., Giuseffi, M., Giglio, E., Sabato, C., Sanseverino, F., & Marino, G. (2024). Synergic role of dietary bioactive compounds in breast cancer chemoprevention and combination therapies. *Nutrients*, 16(12), 1883. <https://doi.org/10.3390/nu16121883>
- Menon, G., Alkabbani, F. M., & Ferguson, T. (2024, February 25). *Breast cancer*. *StatPearls - NCBI Bookshelf*. <https://www.ncbi.nlm.nih.gov/books/NBK482286/>
- Montemayor, Ma. T. (2023, October 6). 65% of breast cancer cases in PH diagnosed in advanced stage. *Philippine News Agency*. <https://www.pna.gov.ph/articles/1211314>
- Ngelangel, C. A., & Wang, E. H. M. (2020). Cancer and the Philippine Cancer Control Program. *Japanese Journal of Clinical Oncology*, 32(suppl 1), S52–S61. <https://doi.org/10.1093/jjco/hye126>
- Novartis. (2021, September 22). Advancements in leukemia treatment: A focus on resource-limited settings. Retrieved from <https://www.novartis.com/ph-en/news/media-releases/world-cml-day-doh-cml-alliance-philippines-novartis-celebrate-two-decades-medical-innovation-new-access-program-cml-patients>
- Olayiwola, Y., & Gollahon, L. (2024). Natural compounds and breast cancer: Chemo-Preventive and therapeutic capabilities of chlorogenic acid and cinnamaldehyde. *Pharmaceuticals*, 17(3), 361. <https://doi.org/10.3390/ph17030361>
- Pires, D. E. V., Blundell, T. L., & Ascher, D. B. (2015). PKCSM: Predicting Small-Molecule Pharmacokinetic and Toxicity Properties Using Graph-Based Signatures. *Journal of Medicinal Chemistry*, 58(9), 4066–4072. <https://doi.org/10.1021/acs.jmedchem.5b00104>
- Pratama, M. R. F., Poerwono, H., & Siswodihardjo, S. (2019). Molecular docking of novel 5-O-benzoylpinostrobin derivatives as wild type and L858R/T790M/V948R mutant EGFR inhibitor. *Journal of Basic and Clinical Physiology and Pharmacology*, 30(6). <https://doi.org/10.1515/jbcpp-2019-0301>
- Roney, M., & Aluwi, M. F. F. M. (2024). The importance of in-silico studies in drug discovery. *Intelligent Pharmacy*. <https://doi.org/10.1016/j.ipha.2024.01.010>

- Rudrapal, M., Khairnar, S. J., & Jadhav, A. G. (2020). Drug repurposing (DR): an emerging approach in drug discovery. *Drug repurposing-hypothesis, molecular aspects and therapeutic applications*, 10.
- Sabilu, Y., & Jafriati, N. (2023). Identification of bioactive compounds of ethanol extract of cayenne pepper (*Capsicum frutescens* L) leaves. *AIP Conference Proceedings*. <https://doi.org/10.1063/5.0138625>
- Sasidharan, S., Chen, Y., Saravanan, D., Sundram, K. M., & Latha, L. Y. (2011). *Extraction, Isolation and Characterization of Bioactive Compounds from Plants' Extracts*. PubMed Central (PMC). <https://www.ncbi.nlm.nih.gov/pmc/articles/PMC3218439/>
- Shrihastini, V., Muthuramalingam, P., Adarshan, S., Sujitha, M., Chen, J., Shin, H., & Ramesh, M. (2021b). Plant derived bioactive compounds, their Anti-Cancer effects and in silico approaches as an alternative target treatment strategy for breast cancer: an updated overview. *Cancers*, 13(24), 6222. <https://doi.org/10.3390/cancers13246222>
- Siegel, R. L., Giaquinto, A. N., & Jemal, A. (2024). Cancer statistics, 2024. *CA a Cancer Journal for Clinicians*, 74(1), 12–49. <https://doi.org/10.3322/caac.21820>
- Stanzione, F., Giangreco, I., & Cole, J. C. (2021). Use of molecular docking computational tools in drug discovery. *Progress in Medicinal Chemistry*, 273–343. <https://doi.org/10.1016/bs.pmch.2021.01.004>
- Tannin-Spitz, T., Grossman, S., Dovrat, S., Gottlieb, H. E., & Bergman, M. (2007). Growth inhibitory activity of cucurbitacin glucosides isolated from *Citrullus colocynthis* on human breast cancer cells. *Biochemical Pharmacology*, 73(1), 56–67. <https://doi.org/10.1016/j.bcp.2006.09.012>
- Tao, B., Wang, D., Yang, S., Liu, Y., Wu, H., Li, Z., ... & Liu, W. (2021). Cucurbitacin B inhibits cell proliferation by regulating X-inactive specific transcript expression in tongue cancer. *Frontiers in Oncology*, 11, 651648.
- Tian, W., Chen, C., Lei, X., Zhao, J., & Liang, J. (2018). CASTp 3.0: computed atlas of surface topography of proteins. *Nucleic Acids Research*, 46(W1), W363–W367. <https://doi.org/10.1093/nar/gky473>
- Trott, O., & Olson, A. J. (2009). AutoDock Vina: Improving the speed and accuracy of docking with a new scoring function, efficient optimization, and multithreading. *Journal of Computational Chemistry*, 31(2), 455–461. <https://doi.org/10.1002/jcc.21334>
- Wang, Wu, W., & Wang, R. (2024). Structure-based, deep-learning models for protein-ligand binding affinity prediction. *Journal of Cheminformatics*, 16(1). <https://doi.org/10.1186/s13321-023-00795-9>
- Wang, X., Su, P., Hao, Q., Zhang, X., Xia, L., & Zhang, Y. (2022). A Chinese classical prescription Guizhi-Fuling Wan in treatment of ovarian cancer: An overview. *Biomedicine & Pharmacotherapy*, 153, 113401. <https://doi.org/10.1016/j.biopha.2022.113401>
- Website, N. (2024, September 10). *Symptoms of breast cancer in women*. nhs.uk. <https://www.nhs.uk/conditions/breast-cancer-in-women/symptoms-of-breast-cancer-in-women/>
- World Health Organization: WHO & World Health Organization: WHO. (2024, March 13). *Breast cancer*. <https://www.who.int/news-room/fact-sheets/detail/breast-cancer#:~:text=Breast%20cancer%20is%20a%20disease,producing%20lobules%20of%20the%20breast>
- Yap, R. V., Marquez, D. L., & De La Serna, F. M. (2023). Young Filipino breast cancer patients have worse survival outcomes. *Ecancermedicalscience*, 17. <https://doi.org/10.3332/ecancer.2023.1639>
- Zhang, L., Wang, Y., & Li, J. (2020). Pharmacological effects of *Momordica charantia*: A review. *Journal of Ethnopharmacology*, 299, 115658.